ARTICLE

Experimental Investigation on Fracturing Behaviors after Liquid Nitrogen Pre-Injection in High-Temperature Sandstone

Decheng Li[1], Yan Zhang[2], Dongdong Ma[2], Haozhe Geng[1] and Yu Wu[1,2,*]

[1]School of Mechanics and Civil Engineering, China University of Mining and Technology, Xuzhou, 221116, China

[2]State Key Laboratory for Geomechanics and Deep Underground Engineering, China University of Mining and Technology, Xuzhou, 221116, China

*Corresponding Author: Yu Wu. Email: wuyu@cumt.edu.cn

ABSTRACT

The fracturing process of sandstone is inherently complex due to its loose internal structure and deformation adaptability. Liquid nitrogen pre-injection has emerged as a promising approach to damage reservoir rocks, effectively reducing fracture pressure and establishing intricate fracture networks, thus offering a potential solution for reservoir reconstruction. To unravel the fundamental mechanisms governing sandstone fracturing behaviors following liquid nitrogen pre-injection, sandstone fracturing experiments were conducted under varying durations of liquid nitrogen injection, rock temperature, and in-situ stress conditions. The experiments showcased the evolution of injection pressure and fracture characteristics under different testing conditions, complemented by electron microscope analysis to elucidate the factors driving the complex fracture characteristics of sandstone. The findings revealed a significant decrease in fracture pressure after liquid nitrogen pre-injection, accompanied by a notable increase in the complexity of the fracture network and the roughness of the fracture surface. Moreover, prolonging the duration of liquid nitrogen injection and elevating reservoir temperature further contributed to reducing fracture pressure, consequently enhancing fracture complexity and surface roughness. Conversely, the application of confining pressure amplified fracture pressure while intensifying the degree of fracturing. Notably, the investigation highlighted the increased presence of microcracks in sandstone resulting from liquid nitrogen pre-injection, facilitating fluid diffusion during fracturing and yielding lower fracture pressures, thereby enhancing the effectiveness of sandstone reservoir reformation. The research results can provide theoretical guidance for geothermal reservoir reconstruction.

KEYWORDS

Sandstone; high temperature; liquid nitrogen pre-injection; fracturing behaviors

Nomenclature

N_2	Nitrogen
LN_2	Liquid nitrogen
AE	Acoustic emission
JRC	Joint roughness coefficient

1 Introduction

Geothermal energy resources possess immense potential, offering continuous thermal energy and presenting a safe and environmentally friendly alternative. China, holding approximately one-sixth of the world's geothermal resources, plays a crucial role in future energy supply [1]. Sandstone, a sedimentary rock characterized by primary internal fractures, mineral grains, and numerous pores, remains relatively unaffected by external factors such as high temperature and stress [2]. Although traditional shallow geothermal resource development techniques have matured, the main technical challenge lies in overcoming the high fracture pressure and complex fracturing processes involved in transforming sandstone geothermal reservoirs. Hence, exploring novel reservoir modification methods becomes imperative for enhancing thermal output.

Hydraulic fracturing techniques are currently prevalent for sandstone thermal reservoir reconstruction; however, water-based fracturing fluids exhibit certain limitations [3,4]. These limitations include reduced reservoir heat exchange efficiency due to water locking and environmental concerns related to water-based fracturing fluids. In recent years, Waterless fracturing technologies utilizing liquid nitrogen (LN_2) have gained increasing attention [5] and have been successfully field-tested [6,7]. LN_2, owing to its low-temperature characteristics, facilitates rapid reservoir cooling, thereby promoting crack initiation and propagation within the rock formation [8]. Cai et al. [9] observed that the interaction between LN_2 and coal led to thermal stress and localized stress concentration, resulting in significant damage to the pore structure. Similarly, Li et al. [10] determined that the freeze-thaw effect of LN_2 caused microcracks, increased porosity, and improved permeability in coal rock samples. Furthermore, LN_2 has the potential to mitigate environmental issues associated with water-based fracturing fluids, as it is an inert fluid that minimizes reservoir damage and water consumption.

Numerous scholars have conducted experiments to study the effects of LN_2 freezing damage on rocks, primarily investigating physical and mechanical properties. For instance, Yang et al. [11] subjected high-temperature rocks to fracturing tests after LN_2 immersion, revealing a 9%–51% reduction in fracture pressure, altered temperature gradients, expansion of the microporous structure due to local tensile stresses, and enhanced fracturing efficiency for specimens above 200°C. Gao et al. [12] explored the fracture failure characteristics of sandstone following low-temperature LN_2 treatment, observing low plastic deformation and apparent brittle failure characteristics in the low-temperature samples. Furthermore, Gao et al. [13] examined the structural damage and tensile failure properties of sandstone under three LN_2 cooling states—initial, frozen, and freeze-thaw states—demonstrating that LN_2 treatment influenced the failure mode of sandstone. Qin et al. [14,15] investigated the heat and mass transfer characteristics of circulating LN_2 injected into coal under triaxial stress conditions, noting that heat energy propagated along the fracture direction, forming an extensive fracture network with a larger influence range. The number of freeze-thaw cycles exerted the most significant influence on the petrophysical properties of coal. Additionally, research has been conducted on LN_2 fracturing. Cha et al. [16] simulated low-temperature fracturing under wellbore conditions using a custom test system, which revealed that intense thermal stimulation induced by LN_2 resulted in visible cracks in concrete blocks and microcracks in sandstone. Repeated thermal shocks augmented the fracturing effect by introducing new cracks and enlarging existing ones. Wu et al. [17] designed laboratory equipment for low-temperature fracturing and performed LN_2 pre-injection fracturing experiments on shale. Comparative analysis with N_2 fracturing samples illustrated that LN_2 pre-injection effectively reduced shale fracture pressure, with a more pronounced impact on the bedding plane compared to the vertical layer. Previous studies on LN_2 fracturing have primarily focused on the physical and mechanical properties of rocks following LN_2 freezing damage. Limited research has been conducted on the actual process of LN_2 fracturing, and little is known about the critical control mechanisms

of LN_2 fracturing. The attention of research on LN_2 fracturing is focused on the change of fracture pressure. Comprehensive analysis of fracture morphology and surface roughness after fracturing remains scarce.

In this study, we aim further to investigate the fracture behavior of sandstone after LN_2 fracturing. To achieve this, we developed a real-time, high-temperature LN_2 pre-injection N_2-assisted fracturing device for conducting LN_2 fracturing experiments on sandstone specimens. The fracture pressure, crack morphology, and fracture surface morphology of sandstone under the action of LN_2 damage and N_2 pressure were obtained by the experiments. Based on the experimental results, the effects of the duration of LN_2 pre-injection, the initial temperature of the reservoir, and *in-situ* stress on the fracture behavior of the sandstone were analyzed. The results can provide theoretical guidance for further research on LN_2 fracturing technology.

2 Laboratory Studies

2.1 Sandstone Specimen

The specimen selected for the test was yellow sandstone, as shown in Fig. 1, which was processed into a cylinder with a height of 100 mm and a diameter of 50 mm. The surfaces of both ends of the specimen were polished until the surface was smooth and kept parallel to each other. To better simulate the fracture process of sandstone in subsurface reservoirs, a hole was opened at the center of the specimen, the diameter of the specimen hole was set to 6 mm, and the depth of the hole was set to 60 mm for LN_2 injection. The samples were dried before the experiment to eliminate the interference of sandstone moisture content on the test results.
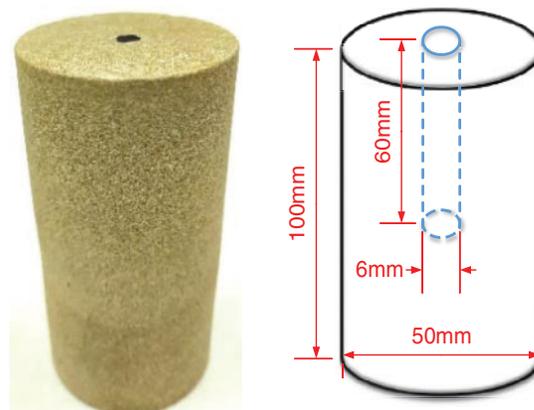

Figure 1: Sandstone sample used in the experiments

2.2 Experimental System

We developed an LN_2 pre-injection fracturing test device to carry out the fracturing test of sandstone after LN_2 pre-injection. The test system consists of an LN_2 pre-injection device (Fig. 2 II), a gas pressurization device (Fig. 2 I), a high-temperature triaxial pressurization device (Fig. 2 III), and a data collection system. The test system can reach a maximum axial pressure and confining pressure of 60 MPa, a maximum temperature of 300°C, and a maximum LN_2 injection rate and pressure of 0.5 L/min and 0.5 MPa, respectively.
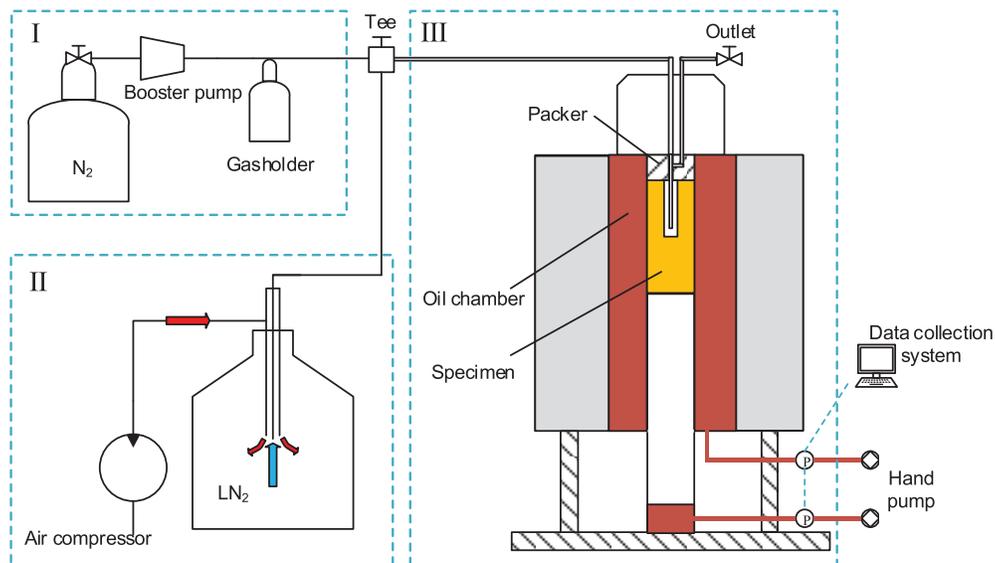
Figure 2: Test systems

2.3 Experimental Methods

To investigate the impact of ultra-low temperature achieved through LN_2 on sandstone fracturing and to further explore the crack morphology and fracture surface characteristics, a series of LN_2 pre-injection fracturing tests were conducted on sandstone samples. The outlet temperature curve during LN_2 pre-injection is illustrated in Fig. 3. The outlet temperature displayed an increase at 10 min, indicating the initiation of the reaction between LN_2 and the rock sample in contact. Subsequently, a sharp drop in temperature at 20 min indicated sufficient reaction between LN_2 and the sample. The temperature change between 20 and 30 min was minimal, suggesting the attainment of internal temperature field equilibrium within the sample. Based on these observations, the duration of LN_2 pre-injection of 10, 20, and 30 min were selected as the time gradients for analysis. To simulate the initial temperature conditions of the geothermal reservoir, reservoir temperature gradients of 100°C, 150°C, and 200°C were selected for the study. Additionally, to assess the effect of in-situ stress variation on the fracturing process, surrounding pressures of 3, 6, and 9 MPa were selected. Detailed experimental conditions for the different samples are provided in Table 1.

Each specimen in the experiment underwent the following procedure. Initially, a preload force of 0.5 kn was applied. Subsequently, the temperature was increased to the preset value and maintained for 30 min. The axial and confining pressures were then incrementally increased to the target values using a manual pump. The experiment was conducted under real-time heating conditions. Afterward, LN_2 was pressurized and transported via a pipeline to the central hole of the sample. Upon contact with the high-temperature sample, LN_2 vaporized and was discharged through the outlet. The air pump was turned off after the designated LN_2 pre-injection time, and when the air pressure in the LN_2 tank reached 0, the three-way valve was reversed while simultaneously closing the outlet valve. N_2 was then injected at a rate of 0.3 L/min. Throughout the experiment, real-time monitoring of pressure, temperature, and other data was performed using a data collection system. A sudden drop in pressure indicated specimen failure. Following the completion of the tests, the fracture surface of each specimen was scanned using the VHX-900F electron microscope to obtain morphological characteristics of the fracture surface.
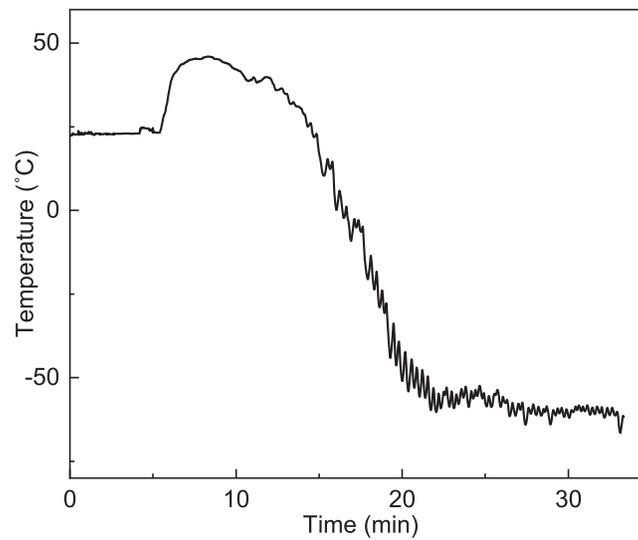
Figure 3: Variation of outlet temperature with time

Table 1: Experimental procedure and sample number

Group experiment	Time (min)	Temperature (°C)	Confining pressure (MPa)	Axial load (MPa)	Sample number
#1	0; 10; 20; 30	100	3	10	L-1; L-2; L-3; L-4
#2	30	100; 150; 200	3	10	L-4; L-5; L-6
#3	30	100	3; 6; 9	10	L-4; L-7; L-8

3 Experimental Results and Analysis

3.1 Effect of LN₂ Cryogenic on Mechanical Properties of Sandstone

Long-term injection of LN_2 can reduce reservoir temperature and change the reservoir environment. Therefore, it is necessary to study the effect of low-temperature LN_2 on the rock. Uniaxial compression tests were performed on sandstone samples subjected to both LN_2 cryogenic treatment and untreated conditions. By incorporating acoustic emission characteristics into the analysis, the relationship between stress, accumulative AE hits, energy, and time during fracturing was examined. The accumulative AE hits serve as an indicator of the level of AE event activity, while the energy measurement reflects the intensity of AE events within the sample.

The compressive strength of the sandstone samples without LN_2 treatment and those treated with LN_2 was measured to be 77.1 and 76.1 MPa, respectively. The variations in stress, accumulative AE hits, and energy over time under different treatment conditions are depicted in Fig. 4. During the initial loading stage, AE events were observed to be associated with the closure of pre-existing microcracks within the rock. As illustrated in Fig. 4a, only a few AE activities were detected in the untreated specimens during the initial loading process. In contrast, the LN_2-treated specimens exhibited significant AE events, indicating that the cooling effect of LN_2 caused some degree of internal structural damage to the rock samples, resulting in the generation of microcracks that gradually closed

under pressure. As the test load increased, the intensity of AE activities peaked near the point of maximum strength. When comparing the untreated samples to the LN$_2$-treated selection, the AE events were more pronounced, indicating a higher degree of sample breakdown. This can be attributed to the damage caused by LN$_2$ cooling and the initiation of microcracks within the sample. As the load continued to increase, cracks expanded and propagated, leading to an increased level of failure.
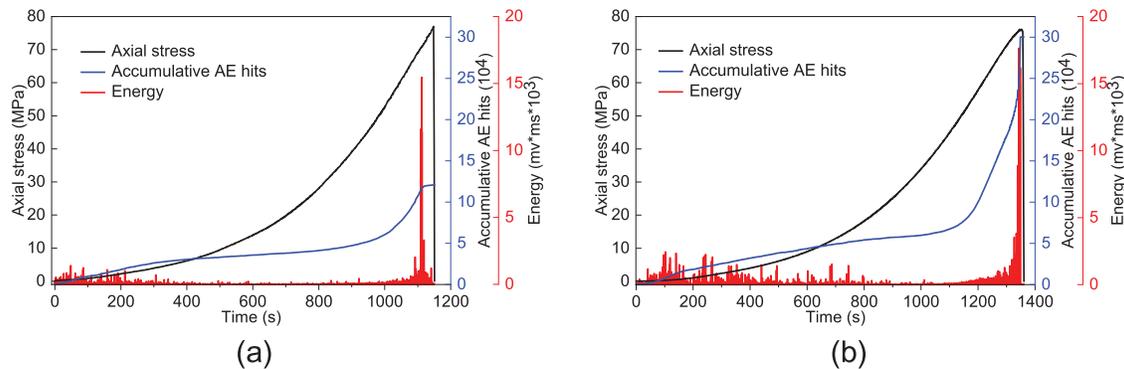

Figure 4: Acoustic emission characteristics. (a) Without LN$_2$ treatment. (b) LN$_2$ treatment

3.2 Breakdown Pressure

Fig. 5 shows the evolution of gas injection pressure with time under different conditions. The breakdown pressure of LN$_2$ pre-injection with 0, 10, 20, and 30 min were 10.62, 5.02, 4.34, and 3.85 MPa, respectively. The sudden and rapid drop in gas injection pressure after reaching its maximum value indicates the occurrence of sample fracture, with the maximum gas injection pressure representing the fracture pressure. Extending the duration of LN$_2$ injection and increasing the temperature both contribute to a decrease in fracture pressure, while higher confining pressure exhibits the opposite effect. In comparison to samples without LN$_2$ pre-injection, the fracture pressure decreased by 52.7% following a 30-min LN$_2$ pre-injection. Notably, when the LN$_2$ injection duration was less than 20 min, the fracture pressure of sandstone exhibited a rapid reduction with increasing injection duration. However, the rate of decrease in fracture pressure slowed down between 20 and 30 min due to the slower temperature drop caused by the internal temperature field reaching equilibrium.

Temperature also plays a significant role in determining fracture pressure. For rock temperatures of 150°C and 200°C, the specific fracture pressure values were measured as 4.25 and 3.85 MPa, respectively. A comparison between the 100°C and 200°C samples reveals a 23.3% decrease in fracture pressure, attributed to the intensified thermal stress caused by LN$_2$ injection at higher temperatures [18]. This thermal stress exerts a more substantial damaging effect on the rock samples. Moreover, an increase in temperature from 100°C to 150°C resulted in a 15.3% decrease in fracture pressure, while a further increase from 150°C to 200°C led to a 9.4% reduction. This diminishing rate of decline may be explained by the occurrence of irreversible plastic deformation in rock minerals at high temperatures, which augments the mechanical properties of the rock [19]. Nonetheless, the decrease in breakdown pressure signifies that the influence of thermal shock resulting from elevated temperature still dominates the fracture process, thereby weakening the mechanical properties of the rock.
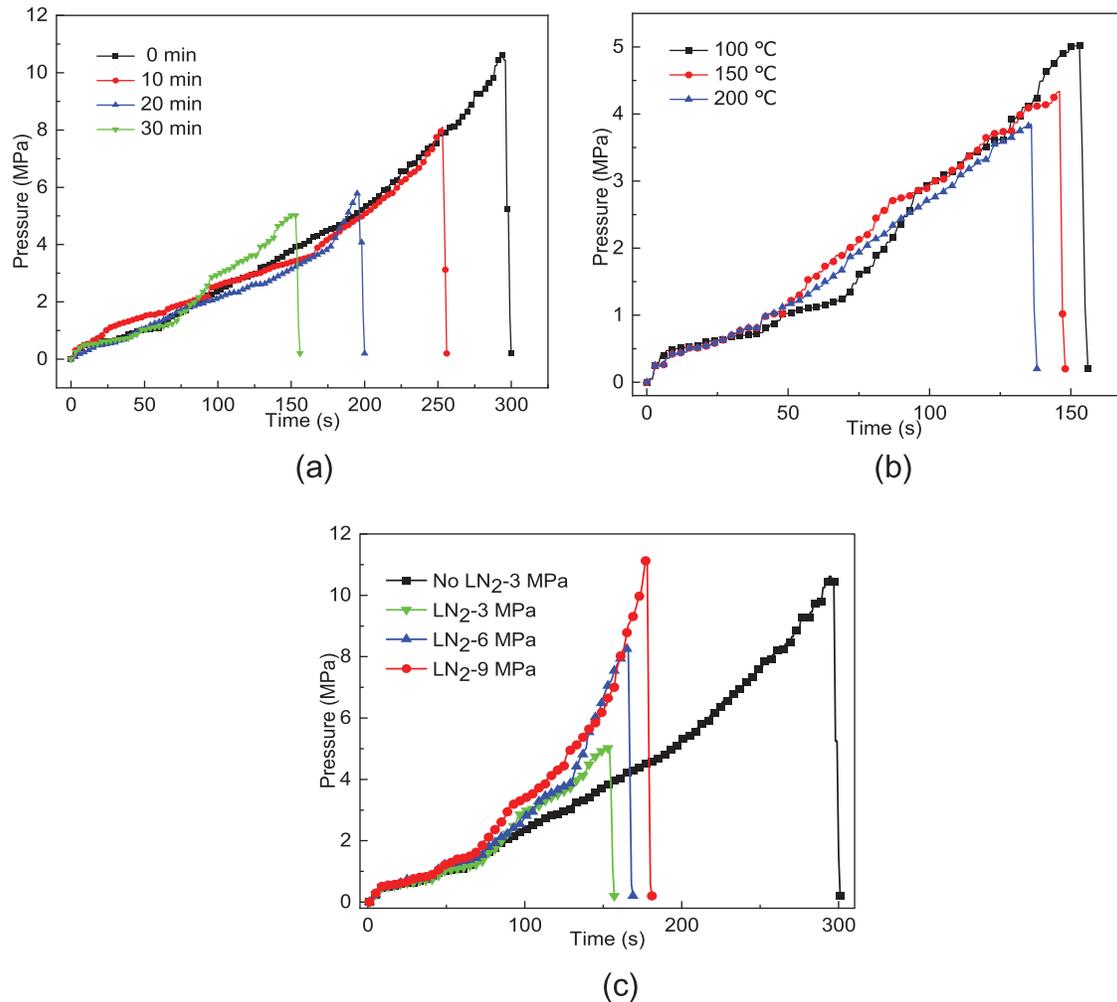
Figure 5: Evolution of gas injection pressure. (a) Duration of the LN_2 injection. (b) Temperature. (c) Confining pressure

The breakdown pressures of the 3, 6, and 9 MPa specimens were 5.02, 8.31, and 11.12 MPa, respectively, while the breakdown pressure of the 3 MPa specimen without liquid nitrogen injection was 10.62 MPa. At a confining loading pressure of 9 MPa, the fracture pressure during sandstone fracturing increased by 54.8% compared to that observed at a confining loading pressure of 3 MPa. This discrepancy can be attributed to the heightened frictional and locking forces between rock mineral particles under higher loading confining pressure, consequently enhancing the macroscopic tensile strength [20] and resulting in an elevation of fracture pressure. However, when comparing rock samples subjected to the same 3 MPa confining pressure without LN_2 pre-injection, a 52.7% decrease in breakdown pressure was observed, indicating that LN_2 pre-injection can still mitigate the breakdown pressure under confining pressure. These findings demonstrate the effective reduction of fracture pressure in deep reservoirs through LN_2 pre-injection.

3.3 Fracturing Behaviors

In Fig. 6, the crack patterns of the rock samples under various experimental conditions are depicted, where the primary cracks are represented in red and the secondary cracks in blue. The upper surface of the rock samples containing the drill holes is shown in Fig. 7a. The fracture surface density and tortuosity of the fractured samples were computed following the method outlined in reference [21] to assess the fracture characteristics. The fracture surface density quantifies the number of fractures on the upper surface of the sandstone after fracturing, while the crack tortuosity evaluates the degree of lateral bending of the specimen's fractures, as illustrated in Fig. 8. In order to analyze the morphological characteristics of the fracture surface, we use the electron microscope to scan the end of the hole of the fracture surface shown in Fig. 9, and the specific scanning position is shown in Fig. 7b. This scanning process defines the lowest point of the fracture surface as 0 height, and the cloud map clearly illustrates the height variations of the scanned portion. The height data at the measured line can be obtained, and the joint roughness coefficient (JRC) is calculated by the method proposed by Tse et al. [22] to characterize the roughness of the fractured surface. The roughness variation under different experimental conditions is shown in Fig. 10. The crack morphology and fracture surface morphological characteristics of the sandstone were used to compare the differences in fracturing behaviors of LN$_2$ fracturing under different conditions.
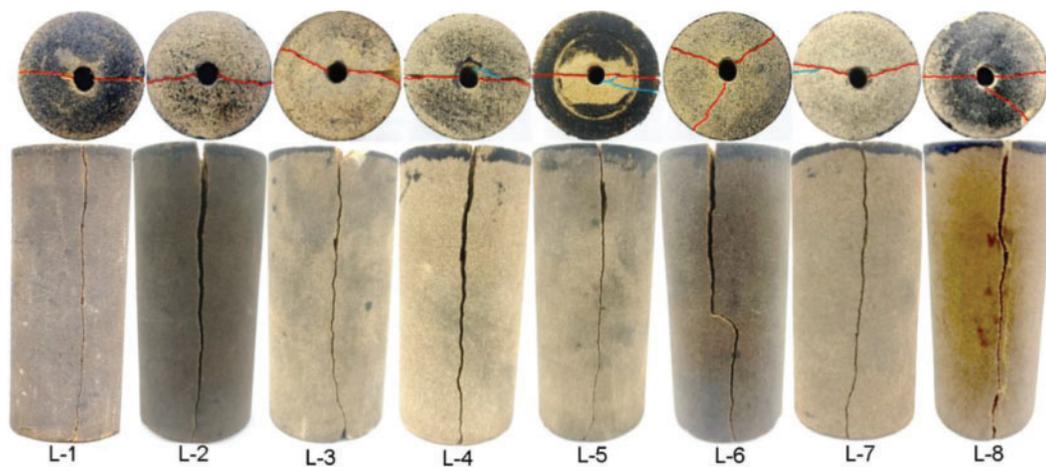

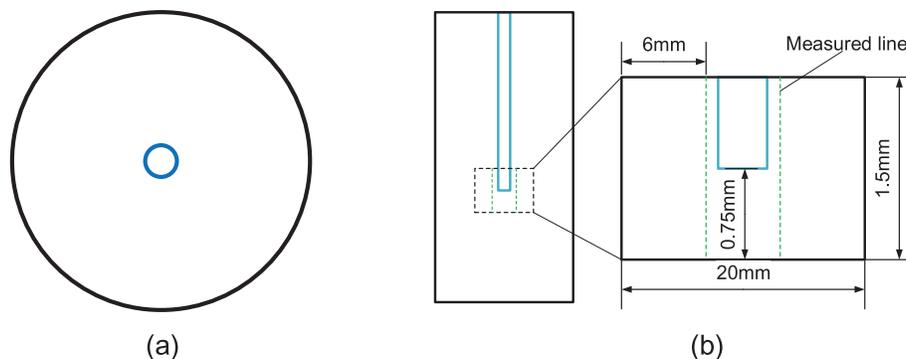**Figure 6:** Crack pattern of specimens

Figure 7: Illustration of specimen position. (a) Upper surface. (b) Scan position
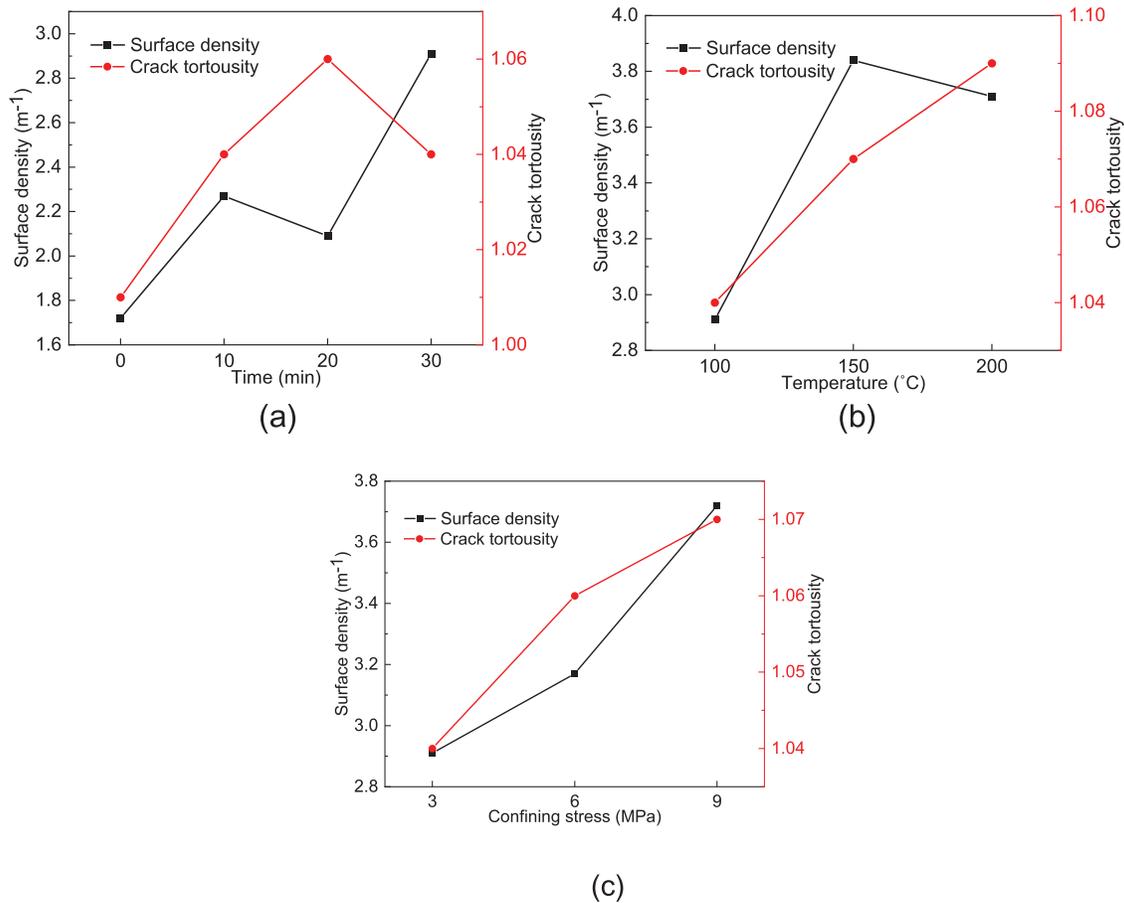
Figure 8: Crack complexity parameters under different conditions. (a) Duration of the LN_2 injection. (b) Temperature. (c) Confining pressure

3.3.1 Fracturing Behaviors of Sandstone under the Different Duration of the LN_2 Injection

The effect of LN_2 injection duration on crack morphology can be observed by examining samples L-1, L-2, L-3, and L-4 in Fig. 6. In the absence of LN_2 pre-injection, the upper surface of the sample exhibits a typical double-wing fracture pattern. A central crack perpendicular to the surface is visible on the side contour of the sample, indicating tensile failure. As the duration of LN_2 injection increases, secondary cracks appear on the upper surface, and the degree of bending in the side cracks intensifies. This change is evident from Fig. 8a, where the fracture surface density and tortuosity demonstrate an increasing trend with longer LN_2 injection duration. These findings suggest that LN_2 pre-injection enhances the complexity of the fracture network, primarily attributed to the strong thermal shock caused by LN_2 injection and the low-temperature effect of LN_2. The substantial thermal stresses resulting from the significant temperature difference between LN_2 injection and high-temperature sandstone can initiate existing cracks within the specimen. Prolonged LN_2 pre-injection creates a low-temperature zone within the reservoir, and the low-temperature effect causes the inward shrinkage of rock particles, leading to the opening and further expansion of microcracks [23]. Figs. 9a and 9b illustrate the fracture surface morphology characteristics for different duration of LN_2 pre-injection. The sample pre-injected with LN_2 for 0 min exhibits a relatively intact fracture surface, whereas the

sample pre-injected with LN_2 for 30 min displays increased roughness on the fracture surface, with crack initiation observed on the hole wall, resulting in an increased JRC. Thus, compared to N_2 fracturing, LN_2 pre-injection effectively enhances fracture complexity and increases the volume of the crack network, thereby facilitating reservoir reconstruction.
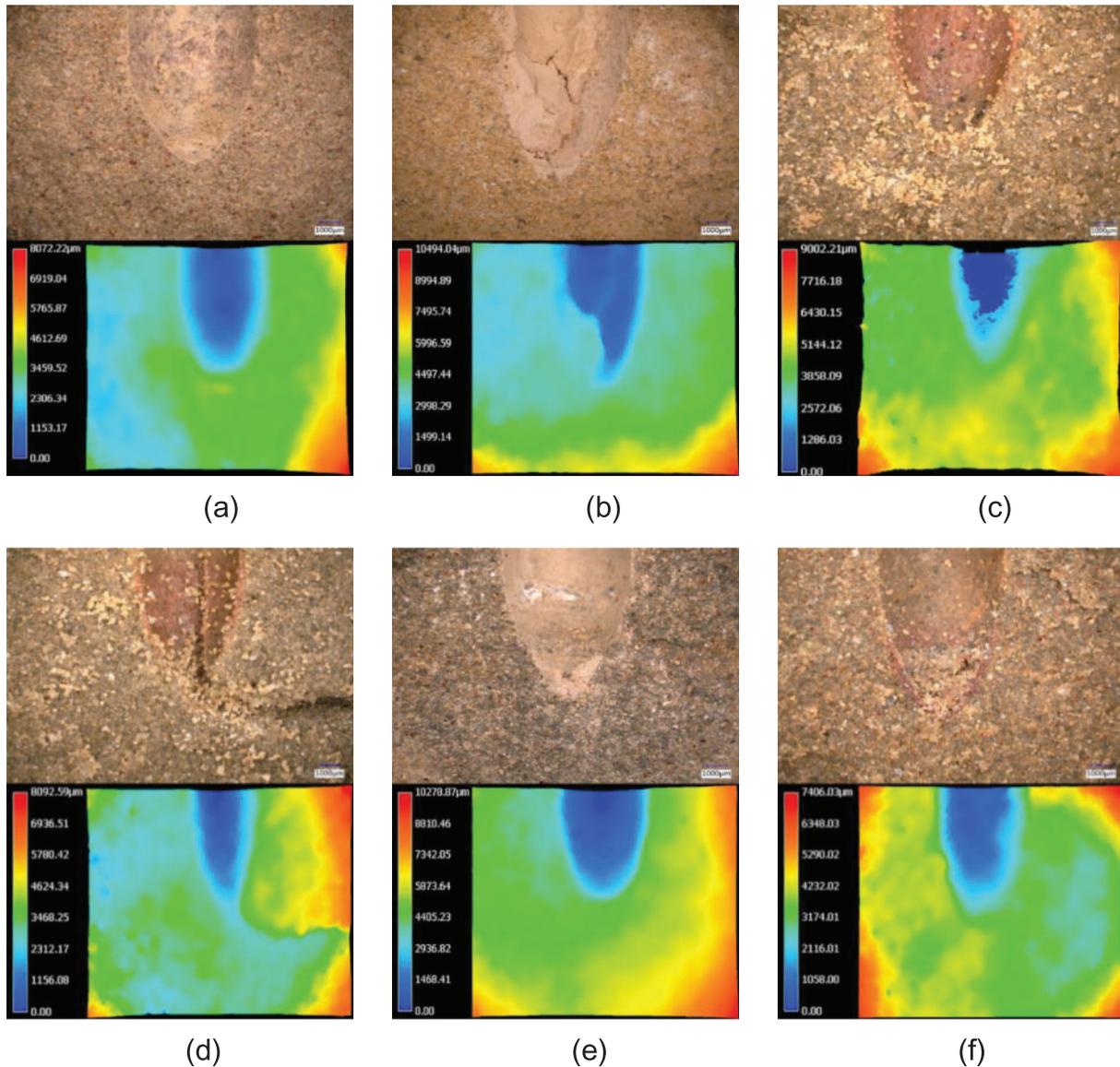

Figure 9: Breakdown of surface morphological characteristics under different conditions. (a) LN_2 pre-injection 0 min. (b) LN_2 pre-injection 30 min. (c) Temperature 150°C. (d) Temperature 200°C. (e) Confining pressure 6 MPa. (f) Confining pressure 9 MPa
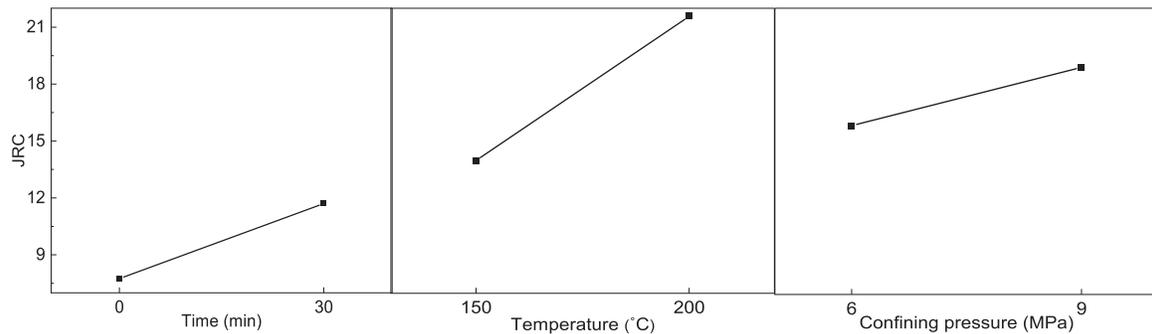
Figure 10: Joint roughness coefficient under different experimental conditions

3.3.2 Fracturing Behaviors of Sandstone under Different Temperature

By examining specimens labeled L-4, L-5, and L-6 in Fig. 6, we can investigate the influence of different rock temperatures on crack morphology. The apparent crack morphology of the samples is significantly affected by varying rock temperatures. Primarily, the specimens exhibit tensile failures. As the temperature increases, the tortuosity of side cracks gradually increases, and the presence of secondary cracks on the upper surface becomes more pronounced. Notably, the 200°C specimen displays three prominent cracks on the upper surface, accompanied by horizontal cracks on the side. Fig. 8b illustrates that crack tortuosity and surface density generally increase with rising temperature, indicating that higher temperatures contribute to enhanced crack density and crack length. This phenomenon is primarily associated with thermal damage and thermal stress resulting from elevated temperature. The high temperature weakens the cementation between sandstone particles, giving rise to the generation of microcracks and internal damage within the sample [11]. As temperature increases, thermal stress also escalates, and the combined effect of these factors leads to more complex crack morphology in the specimens. A comparison of Figs. 9c and 9d reveal the presence of numerous particles on both fracture surfaces. The 200°C specimen exhibits vertical cracks traversing the specimen, and the JRC increases. These results suggest that higher temperatures contribute to increased roughness of the fracture surface and enhance the effectiveness of fracturing. Consequently, LN_2 fracturing holds the potential for the reconstruction of high-temperature reservoirs.

3.3.3 Fracturing Behaviors of Sandstone under Different Stress States

The crack morphology under different in-situ stress conditions can be examined by comparing specimens labeled as L-4, L-7, and L-8 in Fig. 6. All three specimens generally display typical double-wing fractures, with lateral cracks primarily exhibiting tensile accompanied by shear damage. Notably, when the confining loading pressure is 9 MPa, an additional major crack emerges on the upper surface. Fig. 8c demonstrates that both crack tortuosity and surface density increase with rising confining pressure, indicating that elevated confining pressure enhances crack complexity. This phenomenon is primarily attributed to the damage inflicted on the rock by LN_2 pre-injection and the strengthening effect of confining pressure. Increasing the confining pressure improved the cohesion within the sample, resulting in a tighter bond between sandstone particles and enhanced mechanical properties. Consequently, the fracture pressure increases and a greater amount of energy is released during fracture. The thermal shock and low-temperature impact caused by LN_2 pre-injection lead to an increased number of microcracks, enabling rapid expansion along the cracks upon sample failure. This variation intensifies the degree of fracture and generates more complex cracks. A comparison of

Figs. 9e and 9f illustrates that the fracture surface of the sample exhibits more significant fluctuation under a confining loading pressure of 9 MPa, accompanied by evident fracture traces. Additionally, the JRC increases, as depicted in Fig. 10. These results indicate that increasing the confining pressure enhances the degree of sample fracture and the roughness of the fracture surface. Consequently, LN_2 fracturing holds potential for deep reservoir reconstruction, as it can be applied to induce complex fractures under elevated confining pressures.

4 Discussion

LN_2 possesses a significant advantage over other fracturing fluids due to its low-temperature properties, which can cause interior damage to rocks through thermal shock and low-temperature effects. Wu et al. [19] found that LN_2 cooling can affect the mechanical properties of rock, and microcracks are generated inside the rock sample. Sha et al. [24] believed that LN_2 thermal shock damage to rock mainly comes from the expansion of primary cracks and the generation of new cracks caused by thermal stress. The shrinkage deformation of mineral particles during LN_2 pre-injection plays a crucial role in generating these microcracks. Sandstone, composed mainly of quartz and plagioclase, with quartz being the dominant component [25], exhibits heterogeneous thermal conductivity and thermal expansion coefficients. Quartz has a notably higher thermal expansion coefficient compared to other minerals. This heterogeneity causes varying degrees of shrinkage and expansion among different minerals during temperature changes, amplifying local thermal stress and facilitating the opening and expansion of microcracks. The increased presence of microcracks affects the fracture pattern, and when these micro cracks are fully developed and interconnected, it can lead to the formation of additional, prominent cracks, as observed in specimens L-6 and L-8.

During the LN_2 pre-injection process, thermal shock occurs due to the temperature difference between LN_2 and high-temperature sandstone samples, resulting in rock shrinkage and the generation of high tensile stress. If the tensile stress surpasses the tensile strength of sandstone, fracture occurs. Furthermore, LN_2 injection into the reservoir establishes a low-temperature zone. As the duration of LN_2 injection increases, the extent of the low-temperature zone expands, leading to an escalation of thermal stress. The shrinkage and deformation of sandstone particles under low temperatures promote the expansion of microcracks and pore connectivity within the sandstone, enhancing fluid penetration into the rock's interior. Additionally, LN_2 exhibits low viscosity. Once the LN_2 pre-injection is complete, closing the outlet valve triggers a phase change from LN_2 to N_2 due to the high-temperature environment. This phase transition generates expansion forces that further facilitate crack growth [26]. Under fluid pressure, these microcracks are more prone to expansion and interconnection, resulting in increased fracture complexity and surface roughness during rock failure.

5 Conclusion

(1) In this study, real-time high-temperature LN_2 pre-injection N_2-assisted fracturing experiments were conducted to investigate the efficacy of LN_2 pre-injection in addressing the challenges of unsatisfactory fracturing effect and high fracture pressure in sandstone. The findings revealed that compared to conventional N_2, LN_2 pre-injection induced internal damage to the sandstone, significantly reducing fracture pressure. The duration of LN_2 injection and rock temperature were identified as influential factors in reducing fracture pressure while increasing confining pressure was found to elevate fracture pressure.

(2) An increase in the duration of LN_2 injection was observed to expand the low-temperature zone within the reservoir, thereby intensifying thermal stress and leading to the formation of

more intricate fracture morphology and rougher fracture surfaces. Elevated temperature also contributed to rougher fracture surfaces, increased fracture tortuosity, and the occurrence of secondary fractures, primarily attributed to thermal damage and heightened thermal stresses. Moreover, the augmentation of constraint pressure enhanced the overall hardness of sandstone, allowing for more significant energy accumulation during fracture and more vigorous fracture.

(3) The heterogeneous nature of the rock played a significant role in the observed effects, as the thermal shock and low-temperature impact resulting from LN_2 pre-injection inflicted damage on the rock, thereby contributing to the development of complex fracture patterns during fracturing. Notably, high temperature and high in-situ stress contribute to the formation of intricate fracture networks. Consequently, utilizing LN_2 as a pre-fracturing fluid proves to be an effective approach for the modification of deep high-temperature reservoirs.

Author Contributions: Yu Wu: Ideas, Methodology; Decheng Li: Conducting a Research and Investigation Process, Writing-Original Draft, Preparation; Yan Zhang: Methodology, Preparation; Dongdong Ma: Specifically Critical Review; Haozhe Geng: Preparation.

Availability of Data and Materials: The data used to support the findings of this study are available from the corresponding author upon request.

Conflicts of Interest: The authors declare that they have no conflicts of interest to report regarding the present study.

References

1. Wang, G., Zhang, W., Ma, F., Lin, W., Liang, J. et al. (2018). Overview on hydrothermal and hot dry rock researches in China. *China Geology, 1(2),* 273–285.
2. Liu, S., Xu, J. (2015). An experimental study on the physico-mechanical properties of two post-high-temperature rocks. *Engineering Geology, 185,* 63–70.
3. Holtsclaw, J., Loveless, D., Saini, R., Fleming, J. (2011). Environmentally focused crosslinked-gel system results in high retained proppant-pack conductivity. SPE-146832-MS.
4. Javadpour, F., McClure, M., Naraghi, M. E. (2015). Slip-corrected liquid permeability and its effect on hydraulic fracturing and fluid loss in shale. *Fuel, 160,* 549–559.
5. Huang, Z., Zhang, S., Yang, R., Wu, X., Li, R. et al. (2020). A review of liquid nitrogen fracturing technology. *Fuel, 266,* 117040.
6. Grundmann, S. R., Rodvelt, G. D., Dials, G. A., Allen, R. E. (1998). Cryogenic nitrogen as a hydraulic fracturing fluid in the devonian shale. *SPE Eastern Regional Meeting*, Pittsburgh, USA.
7. McDaniel, B. W., Grundmann, S. R., Kendrick, W. D., Wilson, D. R., Jordan, S. W. (1997). Field applications of cryogenic nitrogen as a hydraulic fracturing fluid. *SPE Annual Technical Conference and Exhibition*, San Antonio, USA.
8. Kim, K. M., Kemeny, J. M. (2009). Effect of thermal shock and rapid unloading on mechanical rock properties. *Proceedings of the 43rd US Rock Mechanics Symposium & 4th US-Canada Rock Mechanics Symposium*, Asheville, USA.

9. Cai, C., Li, G., Huang, Z., Shen, Z., Tian, S. (2014). Rock pore structure damage Due to freeze during liquid nitrogen fracturing. *Arabian Journal for Science and Engineering, 39(12),* 9249–9257.

10. Li, B., Zhang, L., Wei, J., Ren, Y. (2018). Pore damage properties and permeability change of coal caused by freeze-thaw action of liquid nitrogen. *Advances in Civil Engineering, 2018,* 1–9.

11. Yang, R., Huang, Z., Shi, Y., Yang, Z., Huang, P. (2019). Laboratory investigation on cryogenic fracturing of hot dry rock under triaxial-confining stresses. *Geothermics, 79,* 46–60.

12. Gao, F., Cai, C., Yang, Y. (2018). Experimental research on rock fracture failure characteristics under liquid nitrogen cooling conditions. *Results in Physics, 9,* 252–262.

13. Gao, Y., Hou, P., Su, S., Wang, S., Liang, X. et al. (2022). Role of liquid nitrogen cooling state in physical and tensile properties of sandstone. *International Journal of Thermophysics, 43(4),* 52.

14. Qin, L., Zhai, C., Liu, S., Xu, J. (2018). Infrared thermal image and heat transfer characteristics of coal injected with liquid nitrogen under triaxial loading for coalbed methane recovery. *International Journal of Heat and Mass Transfer, 118,* 1231–1242.

15. Qin, L., Zhai, C., Liu, S., Xu, J., Wu, S. et al. (2018). Fractal dimensions of low rank coal subjected to liquid nitrogen freeze-thaw based on nuclear magnetic resonance applied for coalbed methane recovery. *Powder Technology, 325,* 11–20.

16. Cha, M., Yin, X., Kneafsey, T., Johanson, B., Alqahtani, N. et al. (2014). Cryogenic fracturing for reservoir stimulation—Laboratory studies. *Journal of Petroleum Science and Engineering, 124,* 436–450.

17. Wu, Y., Tao, J., Wang, J., Zhang, Y., Peng, S. (2021). Experimental investigation of shale breakdown pressure under liquid nitrogen pre-conditioning before nitrogen fracturing. *International Journal of Mining Science and Technology, 31(4),* 611–620.

18. Sun, Y., Zhai, C., Xu, J., Yu, X., Cong, Y. et al. (2022). Damage and failure of hot dry rock under cyclic liquid nitrogen cold shock treatment: A non-destructive ultrasonic test method. *Natural Resources Research, 31(1),* 261–279.

19. Wu, X., Huang, Z., Li, R., Zhang, S., Wen, H. et al. (2018). Investigation on the damage of high-temperature shale subjected to liquid nitrogen cooling. *Journal of Natural Gas Science and Engineering, 57,* 284–294.

20. Liu, Y., Huang, D., Cen, D., Zhong, Z., Gong, F. et al. (2021). Tensile strength and fracture surface morphology of granite under confined direct tension test. *Rock Mechanics and Rock Engineering, 54(9),* 4755–4769.

21. Cai, C., Tao, Z., Ren, K., Liu, S., Yang, Y. et al. (2021). Experimental investigation on the breakdown behaviours of sandstone due to liquid nitrogen fracturing. *Journal of Petroleum Science and Engineering, 200,* 108386.

22. Tse, R., Cruden, D. M. (1979). Estimating joint roughness coefficients. *International Journal of Rock Mechanics and Mining Sciences & Geomechanics Abstracts, 16(5),* 303–307.

23. Cai, C., Gao, F., Yang, Y. (2018). The effect of liquid nitrogen cooling on coal cracking and mechanical properties. *Energy Exploration & Exploitation, 36(6),* 1609–1628.

24. Sha, S., Rong, G., Chen, Z., Li, B., Zhang, Z. (2020). Experimental evaluation of physical and mechanical properties of geothermal reservoir rock after different cooling treatments. *Rock Mechanics and Rock Engineering, 53(11),* 4967–4991.

25. Wu, X., Huang, Z., Zhang, S., Cheng, Z., Li, R. et al. (2019). Damage analysis of high-temperature rocks subjected to LN_2 thermal shock. *Rock Mechanics and Rock Engineering, 52(8),* 2585–2603.

26. Huang, Z., Wu, X., Li, R., Zhang, S., Yang, R. (2019). Mechanism of drilling rate improvement using high-pressure liquid nitrogen jet. *Petroleum Exploration and Development, 46(4),* 810–818.